

HAC: Hash-grid Assisted Context for 3D Gaussian Splatting Compression

Supplementary Material

Yihang Chen^{1,2}, Qianyi Wu², Weiyao Lin^{1*},
Mehrtash Harandi², and Jianfei Cai²

¹ Shanghai Jiao Tong University

² Monash University

{yihchen.ee, wylin}@sjtu.edu.cn,

{qianyi.wu, mehrtash.harandi, jianfei.cai}@monash.edu

Abstract. This is the supplementary material for our paper. Herein, we offer more details of implementations, an extra experiment, quantitative per-scene results across all datasets, and a comprehensive notation table.

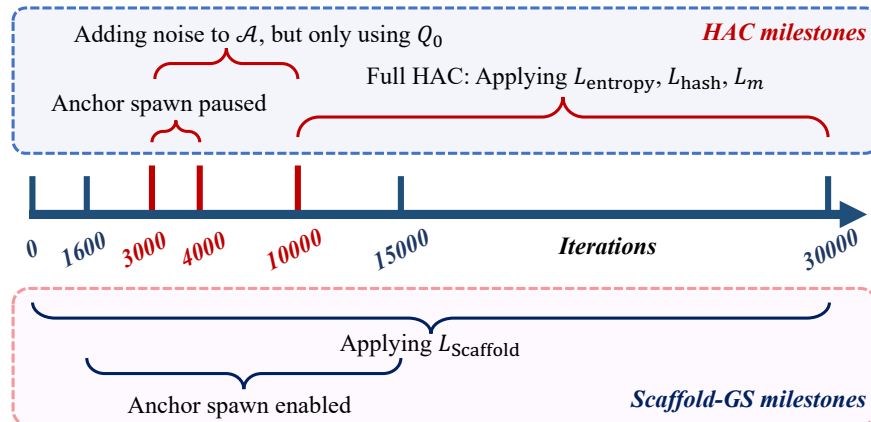


Fig. 1: Detailed training process of our HAC model. We use the [blue box](#) to indicate the training process related to our model, while using the [pink box](#) for Scaffold-GS [5].

1 More Implementation Details

1.1 Training Process

We provide a detailed overview of the training process for our HAC framework, as illustrated in Fig. 1.

* Corresponding author

Table 1: Bit allocation among anchor’s attributes. We set $\lambda_e = 4e - 3$. When calculating per-param size, we only consider *valid* anchors that are not pruned.

| Dataset | Total size (MB) | | | Per-param size (bit) | | |
|--------------------|-----------------|------|------|----------------------|------|------|
| | f^a | l | o | f^a | l | o |
| Bungee-NeRF [7] | 8.76 | 2.53 | 3.62 | 3.03 | 7.27 | 4.56 |
| Synthetic-NeRF [6] | 0.31 | 0.09 | 0.12 | 1.33 | 3.58 | 3.76 |

During the initial 3000 iterations, no additional techniques are applied to impact the original training process of Scaffold-GS [5], ensuring a stable start of the anchor attribute training and anchor spawning.

From iteration 3000 to 10000, we introduce “adding noise” operations to anchor attributes \mathcal{A} , which allows the model to adapt to the quantization process. Note that, in this stage, we only apply Q_0 for quantization without using r for refinement, therefore, we do not need the hash grid. Specifically, we pause the anchor spawning process between iterations 3000 and 4000 for a transitional period, as the sudden introduction of quantization may introduce instability to the spawning process. Once the parameters are fitted to the quantization after iteration 4000, we re-enable the spawning process. Note that we do not incorporate the hash grid in this stage (*i.e.*, before iteration 10000) because we want to provide a transition for the anchor attributes and the spawning process to fit the quantization operation, enabling a more stable training process when the hash grid is incorporated in the further iterations.

After iteration 10000, assuming the 3D model is adequately fitted to the quantization, we fully integrate our HAC framework to jointly train the binary hash grid. Notably, the bound of the hash grid is determined using the maximum and minimum anchor locations at the 10000th iteration, which are then utilized to normalize anchor locations for interpolation in the hash grid. This comprehensive pipeline ensures a stable training process to reduce the model size via entropy constraints while maintaining a high-quality fidelity.

1.2 Sampling Strategy

During training, employing all anchors for entropy training in each iteration could result in prolonged training time and potential out-of-memory (OOM) issues. Therefore, we adopt a sampling strategy that, in each iteration, we only randomly sample and entropy train 5% of anchors from those used for rendering. This approach ensures faster training speeds while still preserving satisfactory RD performance.

2 Additional Experiments

We investigate bit allocation among the anchor’s three attributes, as depicted in Tab. 1. When viewing from the total size, feature f^a contributes the most

due to its highest dimensionality. However, as it needs to be inputted into MLPs to extract Gaussian attributes, it exhibits the most significant dimensional redundancy, resulting in the smallest per-parameter bit. Conversely, this is not the case for scaling \mathbf{l} and offsets \mathbf{o} , which are directly used for rendering, making much fewer dimensional redundancies. Additionally, as \mathbf{l} and \mathbf{o} are always of higher decimal precision, their value distributions are more difficult to accurately predict, resulting higher per-parameter bit consumption.

3 Quantitative Results of Each Scene

3.1 Detailed Results of Our HAC Framework

Detailed per-scene results of Synthetic-NeRF dataset [6] are given in Tab. 2.

Detailed per-scene results of Mip-NeRF360 dataset [1] are given in Tab. 3.

Detailed per-scene results of Tank&Temples dataset [4] are given in Tab. 4.

Detailed per-scene results of DeepBlending dataset [2] are given in Tab. 5.

Detailed per-scene results of BungeeNeRF dataset [7] are given in Tab. 6.

3.2 Detailed Results of the Base Models

We also give detailed per-scene results of all datasets of our two base models 3DGS [3] and Scaffold-GS [5] in Tab. 7 and Tab. 8, respectively.

4 Notation Table

Please refer to Tab. 9 for detailed notation explanations.

Table 2: Per-scene results of Synthetic-NeRF dataset [6] of our approach.

| λ_e | Scenes | PSNR↑ | SSIM↑ | LPIPS↓ | SIZE↓ |
|-------------|------------|--------------|--------------|--------------|-------------|
| 0.004 | chair | 34.02 | 0.981 | 0.018 | 0.82 |
| | drums | 26.20 | 0.950 | 0.044 | 1.23 |
| | ficus | 34.27 | 0.983 | 0.016 | 0.71 |
| | hotdog | 36.44 | 0.979 | 0.033 | 0.51 |
| | lego | 34.25 | 0.976 | 0.027 | 0.97 |
| | materials | 30.20 | 0.959 | 0.045 | 1.07 |
| | mic | 35.39 | 0.989 | 0.011 | 0.55 |
| | ship | 31.24 | 0.902 | 0.124 | 1.82 |
| | AVG | 32.75 | 0.965 | 0.040 | 0.96 |
| 0.003 | chair | 34.33 | 0.982 | 0.017 | 0.89 |
| | drums | 26.26 | 0.951 | 0.043 | 1.42 |
| | ficus | 34.57 | 0.984 | 0.015 | 0.82 |
| | hotdog | 36.70 | 0.980 | 0.031 | 0.54 |
| | lego | 34.65 | 0.977 | 0.024 | 1.07 |
| | materials | 30.29 | 0.960 | 0.043 | 1.20 |
| | mic | 35.62 | 0.990 | 0.010 | 0.62 |
| | ship | 31.32 | 0.903 | 0.121 | 1.86 |
| | AVG | 32.97 | 0.966 | 0.038 | 1.05 |
| 0.002 | chair | 34.73 | 0.984 | 0.016 | 1.03 |
| | drums | 26.32 | 0.952 | 0.043 | 1.45 |
| | ficus | 34.90 | 0.985 | 0.014 | 0.94 |
| | hotdog | 37.11 | 0.981 | 0.029 | 0.64 |
| | lego | 35.04 | 0.979 | 0.022 | 1.25 |
| | materials | 30.53 | 0.961 | 0.041 | 1.45 |
| | mic | 35.92 | 0.990 | 0.010 | 0.67 |
| | ship | 31.38 | 0.903 | 0.119 | 1.99 |
| | AVG | 33.24 | 0.967 | 0.037 | 1.18 |
| 0.001 | chair | 35.21 | 0.985 | 0.014 | 1.32 |
| | drums | 26.38 | 0.952 | 0.041 | 1.95 |
| | ficus | 35.37 | 0.986 | 0.013 | 1.20 |
| | hotdog | 37.47 | 0.983 | 0.026 | 0.79 |
| | lego | 35.51 | 0.981 | 0.019 | 1.61 |
| | materials | 30.58 | 0.961 | 0.040 | 1.62 |
| | mic | 36.25 | 0.991 | 0.009 | 0.81 |
| | ship | 31.48 | 0.904 | 0.116 | 2.50 |
| | AVG | 33.53 | 0.968 | 0.035 | 1.47 |
| 0.0005 | chair | 35.49 | 0.986 | 0.013 | 1.67 |
| | drums | 26.45 | 0.952 | 0.041 | 2.32 |
| | ficus | 35.30 | 0.986 | 0.013 | 1.53 |
| | hotdog | 37.87 | 0.984 | 0.024 | 0.97 |
| | lego | 35.67 | 0.981 | 0.019 | 1.90 |
| | materials | 30.70 | 0.962 | 0.039 | 2.07 |
| | mic | 36.71 | 0.992 | 0.008 | 1.01 |
| | ship | 31.52 | 0.904 | 0.115 | 3.39 |
| | AVG | 33.71 | 0.968 | 0.034 | 1.86 |

Table 3: Per-scene results of Mip-NeRF360 dataset [1] of our approach.

| λ_e | Scenes | PSNR↑ | SSIM↑ | LPIPS↓ | SIZE↓ |
|-------------|------------|--------------|--------------|--------------|--------------|
| 0.004 | bicycle | 25.05 | 0.742 | 0.264 | 27.54 |
| | garden | 27.28 | 0.842 | 0.151 | 22.69 |
| | stump | 26.58 | 0.762 | 0.269 | 18.11 |
| | room | 31.55 | 0.921 | 0.208 | 5.53 |
| | counter | 29.35 | 0.911 | 0.195 | 7.26 |
| | kitchen | 31.16 | 0.923 | 0.131 | 8.05 |
| | bonsai | 32.28 | 0.942 | 0.189 | 8.56 |
| | flower | 21.26 | 0.572 | 0.381 | 19.59 |
| | treehill | 23.30 | 0.645 | 0.356 | 20.04 |
| | AVG | 27.53 | 0.807 | 0.238 | 15.26 |
| 0.003 | bicycle | 25.05 | 0.742 | 0.261 | 30.02 |
| | garden | 27.36 | 0.844 | 0.148 | 24.62 |
| | stump | 26.64 | 0.763 | 0.265 | 19.85 |
| | room | 31.71 | 0.922 | 0.206 | 5.72 |
| | counter | 29.54 | 0.913 | 0.191 | 7.93 |
| | kitchen | 31.22 | 0.925 | 0.128 | 8.84 |
| | bonsai | 32.50 | 0.944 | 0.186 | 9.40 |
| | flower | 21.26 | 0.571 | 0.383 | 20.67 |
| | treehill | 23.26 | 0.645 | 0.356 | 22.08 |
| | AVG | 27.62 | 0.808 | 0.236 | 16.57 |
| 0.002 | bicycle | 25.10 | 0.742 | 0.262 | 33.14 |
| | garden | 27.43 | 0.847 | 0.143 | 27.52 |
| | stump | 26.59 | 0.761 | 0.268 | 21.75 |
| | room | 31.87 | 0.925 | 0.201 | 6.47 |
| | counter | 29.65 | 0.915 | 0.189 | 8.88 |
| | kitchen | 31.46 | 0.928 | 0.125 | 10.05 |
| | bonsai | 32.70 | 0.945 | 0.184 | 10.51 |
| | flower | 21.32 | 0.576 | 0.377 | 23.73 |
| | treehill | 23.34 | 0.647 | 0.350 | 24.83 |
| | AVG | 27.72 | 0.809 | 0.233 | 18.54 |
| 0.001 | bicycle | 25.11 | 0.742 | 0.259 | 39.15 |
| | garden | 27.46 | 0.849 | 0.139 | 32.17 |
| | stump | 26.59 | 0.763 | 0.264 | 25.26 |
| | room | 31.90 | 0.926 | 0.198 | 7.85 |
| | counter | 29.74 | 0.918 | 0.184 | 10.44 |
| | kitchen | 31.63 | 0.930 | 0.122 | 12.07 |
| | bonsai | 32.97 | 0.948 | 0.180 | 12.72 |
| | flower | 21.27 | 0.575 | 0.377 | 27.55 |
| | treehill | 23.26 | 0.648 | 0.345 | 29.65 |
| | AVG | 27.77 | 0.811 | 0.230 | 21.87 |
| 0.0005 | bicycle | 25.05 | 0.742 | 0.258 | 44.01 |
| | garden | 27.50 | 0.850 | 0.139 | 36.27 |
| | stump | 26.57 | 0.762 | 0.264 | 28.93 |
| | room | 32.19 | 0.929 | 0.194 | 9.16 |
| | counter | 29.75 | 0.918 | 0.185 | 12.22 |
| | kitchen | 31.81 | 0.931 | 0.120 | 13.96 |
| | bonsai | 33.16 | 0.949 | 0.178 | 14.90 |
| | flower | 21.28 | 0.575 | 0.376 | 31.24 |
| | treehill | 23.22 | 0.646 | 0.346 | 34.42 |
| | AVG | 27.83 | 0.811 | 0.229 | 25.01 |

Table 4: Per-scene results of Tank&Temples dataset [4] of our approach.

| λ_e | Scenes | PSNR↑ | SSIM↑ | LPIPS↓ | SIZE↓ |
|-------------|------------|--------------|--------------|--------------|--------------|
| 0.004 | truck | 25.88 | 0.878 | 0.158 | 9.26 |
| | train | 22.19 | 0.815 | 0.216 | 6.94 |
| | AVG | 24.04 | 0.846 | 0.187 | 8.10 |
| 0.003 | truck | 25.99 | 0.880 | 0.153 | 9.80 |
| | train | 22.49 | 0.817 | 0.213 | 7.59 |
| | AVG | 24.24 | 0.849 | 0.183 | 8.70 |
| 0.002 | truck | 25.99 | 0.881 | 0.153 | 11.15 |
| | train | 22.66 | 0.819 | 0.210 | 8.64 |
| | AVG | 24.33 | 0.850 | 0.181 | 9.90 |
| 0.001 | truck | 26.02 | 0.883 | 0.147 | 12.42 |
| | train | 22.78 | 0.823 | 0.207 | 10.07 |
| | AVG | 24.40 | 0.853 | 0.177 | 11.24 |
| 0.0005 | truck | 26.00 | 0.883 | 0.146 | 15.12 |
| | train | 22.49 | 0.823 | 0.206 | 11.19 |
| | AVG | 24.25 | 0.853 | 0.176 | 13.16 |

Table 5: Per-scene results of DeepBlending dataset [2] of our approach.

| λ_e | Scenes | PSNR↑ | SSIM↑ | LPIPS↓ | SIZE↓ |
|-------------|------------|--------------|--------------|--------------|-------------|
| 0.004 | playroom | 30.44 | 0.902 | 0.272 | 3.15 |
| | drjohnson | 29.53 | 0.903 | 0.265 | 5.55 |
| | AVG | 29.98 | 0.902 | 0.269 | 4.35 |
| 0.003 | playroom | 30.61 | 0.903 | 0.269 | 3.66 |
| | drjohnson | 29.67 | 0.904 | 0.261 | 5.71 |
| | AVG | 30.14 | 0.903 | 0.265 | 4.69 |
| 0.002 | playroom | 30.66 | 0.905 | 0.265 | 4.12 |
| | drjohnson | 29.69 | 0.905 | 0.258 | 6.51 |
| | AVG | 30.17 | 0.905 | 0.262 | 5.32 |
| 0.001 | playroom | 30.84 | 0.906 | 0.262 | 5.03 |
| | drjohnson | 29.85 | 0.906 | 0.255 | 7.67 |
| | AVG | 30.34 | 0.906 | 0.258 | 6.35 |
| 0.0005 | playroom | 30.66 | 0.906 | 0.259 | 6.08 |
| | drjohnson | 29.76 | 0.906 | 0.255 | 9.09 |
| | AVG | 30.21 | 0.906 | 0.257 | 7.58 |

Table 6: Per-scene results of BungeeNeRF dataset [7] of our approach.

| λ_e | Scenes | PSNR↑ | SSIM↑ | LPIPS↓ | SIZE↓ |
|-------------|------------|--------------|--------------|--------------|--------------|
| 0.004 | amsterdam | 26.80 | 0.865 | 0.224 | 22.49 |
| | bilbao | 27.65 | 0.864 | 0.231 | 17.14 |
| | hollywood | 24.25 | 0.748 | 0.347 | 16.55 |
| | pompidou | 25.16 | 0.829 | 0.266 | 20.40 |
| | quebec | 29.33 | 0.918 | 0.192 | 15.06 |
| | rome | 25.68 | 0.845 | 0.243 | 19.30 |
| | AVG | 26.48 | 0.845 | 0.250 | 18.49 |
| 0.003 | amsterdam | 26.95 | 0.873 | 0.214 | 24.41 |
| | bilbao | 27.82 | 0.872 | 0.218 | 18.76 |
| | hollywood | 24.27 | 0.753 | 0.342 | 17.87 |
| | pompidou | 25.34 | 0.837 | 0.255 | 22.49 |
| | quebec | 29.67 | 0.924 | 0.185 | 16.15 |
| | rome | 25.98 | 0.855 | 0.231 | 20.83 |
| | AVG | 26.67 | 0.852 | 0.241 | 20.08 |
| 0.002 | amsterdam | 27.13 | 0.880 | 0.202 | 27.14 |
| | bilbao | 28.02 | 0.880 | 0.205 | 20.91 |
| | hollywood | 24.43 | 0.763 | 0.330 | 20.09 |
| | pompidou | 25.27 | 0.842 | 0.249 | 24.85 |
| | quebec | 29.98 | 0.929 | 0.175 | 17.90 |
| | rome | 26.28 | 0.866 | 0.219 | 23.07 |
| | AVG | 26.85 | 0.860 | 0.230 | 22.33 |
| 0.001 | amsterdam | 27.25 | 0.886 | 0.190 | 31.84 |
| | bilbao | 27.98 | 0.886 | 0.190 | 24.38 |
| | hollywood | 24.59 | 0.772 | 0.319 | 23.41 |
| | pompidou | 25.58 | 0.851 | 0.236 | 29.19 |
| | quebec | 30.30 | 0.934 | 0.163 | 21.23 |
| | rome | 26.61 | 0.876 | 0.203 | 26.91 |
| | AVG | 27.05 | 0.868 | 0.217 | 26.16 |
| 0.0005 | amsterdam | 27.24 | 0.891 | 0.180 | 36.31 |
| | bilbao | 28.09 | 0.891 | 0.181 | 27.72 |
| | hollywood | 24.60 | 0.778 | 0.313 | 26.00 |
| | pompidou | 25.60 | 0.853 | 0.231 | 33.55 |
| | quebec | 30.19 | 0.936 | 0.155 | 24.56 |
| | rome | 26.73 | 0.881 | 0.194 | 30.21 |
| | AVG | 27.08 | 0.872 | 0.209 | 29.72 |

Table 7: Per-scene results of all evaluated datasets of 3DGS [3].

| Datasets | Scenes | PSNR↑ | SSIM↑ | LPIPS↓ | SIZE↓ |
|----------------|------------|--------------|--------------|--------------|----------------|
| Synthetic-NeRF | chair | 35.65 | 0.988 | 0.010 | 115.77 |
| | drums | 26.28 | 0.955 | 0.037 | 92.87 |
| | ficus | 35.48 | 0.987 | 0.012 | 64.53 |
| | hotdog | 38.05 | 0.985 | 0.020 | 43.37 |
| | lego | 35.98 | 0.982 | 0.017 | 80.53 |
| | materials | 30.48 | 0.960 | 0.037 | 38.50 |
| | mic | 36.76 | 0.993 | 0.006 | 48.31 |
| | ship | 31.73 | 0.907 | 0.107 | 63.82 |
| | AVG | 33.80 | 0.970 | 0.031 | 68.46 |
| | | | | | |
| Mip-NeRF360 | bicycle | 25.11 | 0.746 | 0.245 | 1336.45 |
| | garden | 27.30 | 0.856 | 0.122 | 1327.99 |
| | stump | 26.66 | 0.770 | 0.242 | 1070.92 |
| | room | 31.74 | 0.926 | 0.197 | 353.10 |
| | counter | 29.07 | 0.914 | 0.184 | 277.39 |
| | kitchen | 31.47 | 0.931 | 0.117 | 414.33 |
| | bonsai | 32.12 | 0.946 | 0.181 | 295.33 |
| | flower | 21.36 | 0.588 | 0.360 | 814.24 |
| | treehill | 22.62 | 0.636 | 0.347 | 812.63 |
| | AVG | 27.49 | 0.813 | 0.222 | 744.71 |
| Tank&Temples | truck | 25.38 | 0.877 | 0.148 | 606.99 |
| | train | 22.00 | 0.811 | 0.208 | 254.91 |
| | AVG | 23.69 | 0.844 | 0.178 | 430.95 |
| DeepBlending | playroom | 29.83 | 0.900 | 0.247 | 551.93 |
| | drjohnson | 29.02 | 0.898 | 0.247 | 775.91 |
| | AVG | 29.42 | 0.899 | 0.247 | 663.92 |
| BungeeNeRF | amsterdam | 26.03 | 0.874 | 0.170 | 1458.14 |
| | bilbao | 26.35 | 0.864 | 0.191 | 1350.37 |
| | hollywood | 23.44 | 0.767 | 0.241 | 1601.76 |
| | pompidou | 21.20 | 0.772 | 0.266 | 2169.21 |
| | quebec | 28.83 | 0.923 | 0.156 | 1468.76 |
| | rome | 23.34 | 0.848 | 0.206 | 1649.12 |
| | AVG | 24.87 | 0.841 | 0.205 | 1616.23 |

Table 8: Per-scene results of all evaluated datasets of Scaffold-GS [5].

| Datasets | Scenes | PSNR↑ | SSIM↑ | LPIPS↓ | SIZE↓ |
|----------------|------------|--------------|--------------|--------------|---------------|
| Synthetic-NeRF | chair | 34.96 | 0.985 | 0.013 | 15.50 |
| | drums | 26.36 | 0.949 | 0.045 | 26.93 |
| | ficus | 34.66 | 0.984 | 0.015 | 16.46 |
| | hotdog | 37.82 | 0.984 | 0.022 | 11.31 |
| | lego | 35.48 | 0.981 | 0.018 | 19.84 |
| | materials | 30.37 | 0.958 | 0.043 | 23.12 |
| | mic | 36.37 | 0.991 | 0.008 | 14.83 |
| | ship | 31.27 | 0.896 | 0.119 | 26.90 |
| | AVG | 33.41 | 0.966 | 0.035 | 19.36 |
| | | | | | |
| Mip-NeRF360 | bicycle | 24.50 | 0.705 | 0.306 | 248.00 |
| | garden | 27.17 | 0.842 | 0.146 | 271.00 |
| | stump | 26.27 | 0.784 | 0.284 | 493.00 |
| | room | 31.93 | 0.925 | 0.202 | 133.00 |
| | counter | 29.34 | 0.914 | 0.191 | 194.00 |
| | kitchen | 31.30 | 0.928 | 0.126 | 173.00 |
| | bonsai | 32.70 | 0.946 | 0.185 | 258.00 |
| | flower | 21.14 | 0.566 | 0.417 | 253.00 |
| | treehill | 23.19 | 0.642 | 0.410 | 262.00 |
| | AVG | 27.50 | 0.806 | 0.252 | 253.89 |
| Tank&Temples | truck | 25.77 | 0.883 | 0.147 | 107.00 |
| | train | 22.15 | 0.822 | 0.206 | 66.00 |
| | AVG | 23.96 | 0.853 | 0.177 | 86.50 |
| DeepBlending | playroom | 30.62 | 0.904 | 0.258 | 63.00 |
| | drjohnson | 29.80 | 0.907 | 0.250 | 69.00 |
| | AVG | 30.21 | 0.906 | 0.254 | 66.00 |
| BungeeNeRF | amsterdam | 27.16 | 0.898 | 0.188 | 223.00 |
| | bilbao | 26.60 | 0.857 | 0.257 | 178.00 |
| | hollywood | 24.49 | 0.787 | 0.318 | 155.00 |
| | pompidou | 24.94 | 0.839 | 0.271 | 209.00 |
| | quebec | 30.28 | 0.936 | 0.190 | 159.00 |
| | rome | 26.23 | 0.873 | 0.225 | 174.00 |
| | AVG | 26.62 | 0.865 | 0.241 | 183.00 |

Table 9: Notation Table. With slight abuse of notation, we use L_{3d} and L_{2d} to represent the number of levels of the 3D and 2D part of the hash grid, respectively.

| Notation | Shape | Definition |
|-----------------------|------------------------------------|---|
| \mathbf{x} | \mathbb{R}^3 | A random 3D point |
| $\boldsymbol{\mu}$ | \mathbb{R}^3 | Location of Gaussians in 3DGS [3] |
| $\boldsymbol{\Sigma}$ | $\mathbb{R}^{3 \times 3}$ | Covariance matrix of Gaussians |
| \mathbf{S} | $\mathbb{R}^{3 \times 3}$ | Scale matrix of Gaussians |
| \mathbf{R} | $\mathbb{R}^{3 \times 3}$ | Rotation matrix of Gaussians |
| α | \mathbb{R}^1 | Opacity of Gaussians after 2D projection |
| \mathbf{c} | \mathbb{R}^3 | View-dependent color of Gaussians |
| I | | Number of Gaussians contributed to the rendering |
| \mathbf{C} | \mathbb{R}^3 | The obtained pixel value after rendering |
| \mathbf{x}^a | \mathbb{R}^3 | Anchor location |
| \mathbf{f}^a | \mathbb{R}^{D^a} | Feature of the anchor |
| \mathbf{l} | \mathbb{R}^6 | Scaling of the anchor |
| \mathbf{o} | \mathbb{R}^{3K} | Offsets of the anchor |
| \mathcal{A} | | The set of anchor's attributes including $\{\mathbf{f}^a, \mathbf{l}, \mathbf{o}\}$ |
| D^a | | Dimension of \mathbf{f}^a |
| K | | Number of offsets per anchor |
| \mathcal{H} | | A 3D-2D mixed binary hash grid |
| T | | Table size of the hash grid at each level |
| L | | Number of levels of the hash grid |
| D^h | | Dimension of the vectors of the hash grid |
| $\boldsymbol{\theta}$ | \mathbb{R}^{D^h} | A vector of the hash grid |
| \mathbf{f}^h | $\mathbb{R}^{D^h(L_{3d}+3L_{2d})}$ | Feature obtained by interpolation of \mathbf{x}^a in \mathcal{H} |
| \mathbf{f} | \mathbb{R}^D | Any of anchor's attribute vectors $\in \{\mathbf{f}^a, \mathbf{l}, \mathbf{o}\}$ |
| $\hat{\mathbf{f}}$ | \mathbb{R}^D | Quantized version of \mathbf{f} |
| D | | Dimension of \mathbf{f} , which $\in \{D^a, 6, 3K\}$ |
| q | \mathbb{R}^1 | Quantization step of \mathbf{f} |
| r | \mathbb{R}^1 | Quantization step refinement term |
| $\boldsymbol{\mu}$ | \mathbb{R}^D | Estimated mean value for distribution modeling |
| $\boldsymbol{\sigma}$ | \mathbb{R}^D | Estimated standard deviation for distribution modeling |
| Q_0 | | Base quantization step, which varies for $\mathbf{f}^a, \mathbf{l}, \mathbf{o}$. |
| N | | Total number of anchors |
| h_f | | Occurrence frequency of “+1” in \mathcal{H} |
| M_+ | | Total number of “+1” \mathcal{H} |
| M_- | | Total number of “-1” \mathcal{H} |
| L_{Scaffold} | | The loss item used in Scaffold-GS [5] |
| L_{entropy} | | Entropy loss for measuring bits of \mathcal{A} |
| L_{hash} | | Entropy loss for measuring bits of \mathcal{H} |
| L_m | | Masking loss |
| Loss | | The total loss |
| λ_e | | Tradeoff parameter to achieve variable bitrate |
| λ_m | | Tradeoff parameter to balance masking ratio |
| MLP_a | | The MLP to deduce r from \mathbf{f}^h |
| MLP_c | | The MLP to deduce $\boldsymbol{\mu}$ and $\boldsymbol{\sigma}$ from \mathbf{f}^h |
| ϕ | | Probability density function of Gaussian distribution |
| Φ | | Cumulative distribution function of Gaussian distribution |

References

1. Barron, J.T., Mildenhall, B., Verbin, D., Srinivasan, P.P., Hedman, P.: Mip-nerf 360: Unbounded anti-aliased neural radiance fields. In: Proceedings of the IEEE/CVF Conference on Computer Vision and Pattern Recognition. pp. 5470–5479 (2022)
2. Hedman, P., Philip, J., Price, T., Frahm, J.M., Drettakis, G., Brostow, G.: Deep blending for free-viewpoint image-based rendering. ACM Transactions on Graphics (ToG) **37**(6), 1–15 (2018)
3. Kerbl, B., Kopanas, G., Leimkühler, T., Drettakis, G.: 3d gaussian splatting for real-time radiance field rendering. ACM Transactions on Graphics **42**(4) (2023)
4. Knapitsch, A., Park, J., Zhou, Q.Y., Koltun, V.: Tanks and temples: Benchmarking large-scale scene reconstruction. ACM Transactions on Graphics (ToG) **36**(4), 1–13 (2017)
5. Lu, T., Yu, M., Xu, L., Xiangli, Y., Wang, L., Lin, D., Dai, B.: Scaffold-gs: Structured 3d gaussians for view-adaptive rendering. In: Proceedings of the IEEE/CVF Conference on Computer Vision and Pattern Recognition (2024)
6. Mildenhall, B., Srinivasan, P.P., Tancik, M., Barron, J.T., Ramamoorthi, R., Ng, R.: Nerf: Representing scenes as neural radiance fields for view synthesis. Communications of the ACM **65**(1), 99–106 (2021)
7. Xiangli, Y., Xu, L., Pan, X., Zhao, N., Rao, A., Theobalt, C., Dai, B., Lin, D.: Bungeenerf: Progressive neural radiance field for extreme multi-scale scene rendering. In: European conference on computer vision. pp. 106–122. Springer (2022)